



High CO₂ fluxes from grassland on histic Gleysol along soil carbon and drainage gradients

K. Leiber-Sauheitl¹, R. Fuß^{1,*}, C. Voigt^{1,2,*}, and A. Freibauer^{1,*}

¹Thünen Institute of Climate-Smart Agriculture, Bundesallee 50, 38116 Braunschweig, Germany

²Department of Environmental Science, University of Eastern Finland, P.O. Box 1627, 70211 Kuopio, Finland

*The co-authors contributed equally to this work.

Correspondence to: K. Leiber-Sauheitl (katharina.leiber@ti.bund.de)

Received: 17 June 2013 – Published in Biogeosciences Discuss.: 9 July 2013

Revised: 9 December 2013 – Accepted: 5 January 2014 – Published: 7 February 2014

Abstract. Drained organic soils are anthropogenic emission hotspots of greenhouse gases (GHGs). Most studies have focused on deep peat soils and on peats with high organic carbon content. In contrast, histic Gleysols are characterized by shallow peat layers, which are left over from peat cutting activities or by peat mixed with mineral soil. It is unknown whether they emit less GHGs than deep Histosols when drained. We present the annual carbon and GHG balance of grasslands for six sites on nutrient-poor histic Gleysols with a shallow (30 cm) histic horizon or mixed with mineral soil in Northern Germany (soil organic carbon concentration (C_{org}) from 9 to 52 %).

The net GHG balance, corrected for carbon export by harvest, was around 4 t CO₂-C-eq ha⁻¹ yr⁻¹ on soils with peat layer and little drainage (mean annual water table < 20 cm below surface). The net GHG balance reached 7–9 t CO₂-C-eq ha⁻¹ yr⁻¹ on soils with sand mixed into the peat layer and water tables between 14 cm and 39 cm below surface. GHG emissions from drained histic Gleysols (i) were as high as those from deep Histosols, (ii) increase linearly from shallow to deeper drainage, (iii) but are not affected by C_{org} content of the histic horizon. Ecosystem respiration (R_{eco}) was linearly correlated with water table level even if it was below the histic horizon. The R_{eco} /GPP ratio was 1.5 at all sites, so that we ruled out a major influence of the inter-site variability in vegetation composition on annual net ecosystem exchange (NEE).

The IPCC definition of organic soils includes shallow histic topsoil, unlike most national and international definitions of Histosols. Our study confirms that this broader definition is appropriate considering anthropogenic GHG emissions

from drained organic soils. Countries currently apply soil maps in national GHG inventories which are likely not to include histic Gleysols. The land area with GHG emission hotspots due to drainage is likely to be much higher than anticipated.

Deeply drained histic Gleysols are GHG hotspots that have so far been neglected or underestimated. Peat mixing with sand does not mitigate GHG emissions. Our study implies that rewetting organic soils, including histic Gleysols, has a much higher relevance for GHG mitigation strategies than currently recognized.

1 Introduction

Organic soils constitute three percent of the land area of the temperate zone in Europe (Montanarella et al., 2006; Kottek et al., 2006). A large fraction of them has been drained for forestry, agriculture, and peat extraction. In Germany, organic soils make up approximately five percent of the land area, about 1.7 million ha (UBA, 2012; Richter, 1998) and drainage for agricultural purposes or industrial peat extraction was conducted on nearly all of these soils (UBA, 2012). During cultivation of organic soils, degradation of soil organic substances causes emission of high amounts of CO₂ and often N₂O as well as subsidence of the peat layers (Smith and Conen, 2004). As a result, only shallow peat soils remain in many former peatland areas and many peatlands have even completely disappeared (e.g. 61 % over 30 yr in Denmark, Nielsen et al., 2012). Such loss of peatland areas as carbon

storage significantly contributes to global warming (Limpens et al., 2008).

The dominant land use on peat soils of the European boreal zone is forestry (Drösler et al., 2008), whereas in the temperate zone grassland of varying management intensity predominates (Schrier-Uijl et al., 2010). In laboratory studies, CO₂ emissions from drained peat scale almost linearly with the depth of the aerated soil above the water table (Dinsmore et al., 2009). Peat quality is an important issue concerning CO₂ emissions (Reiche et al., 2010). Due to Blodau (2002) the amount of easily degradable carbon is positively correlated with CO₂, CH₄ and N₂O fluxes. Moreover, mixing peat with mineral subsoil can either result in C loss by mobilization of C_{org} due to an increase of aerated surfaces or result in a reduction of C emissions by C_{org} stabilization on mineral surfaces (Marschner et al., 2008; Mikutta et al., 2006) and/or by C_{org} dilution by mineral soil material (Don et al., 2013).

Most studies focus on peat soils, which meet the definition of Histosols. Histosols are defined as featuring high carbon content (20 to 30 %) and an organic horizon larger than 40 cm (WRB, 2008). The IPCC definition of peat soils is broader and assumes that shallow peat soils (≥ 10 cm) and strongly degraded ones (≥ 12 % C_{org}) also behave like real peat soils concerning GHG fluxes (IPCC, 2006). Most countries ignore soils with a lower organic carbon content in the national GHG inventory and often focus on deep organic soils. In contrast, in the Danish GHG inventory it is assumed that intermediate to typical mineral soils (C_{org} concentration < 6 %) and peat (C_{org} concentration > 12 %) emit half as much GHG as organic soils (Nielsen et al., 2012). However, according to this report no measurements were conducted on these soils.

To fill this data gap and to test the validity of GHG inventory assumptions, we focus on the most common land-use type in temperate climates (grassland) and measure GHGs along drainage and carbon gradients on a heavily degraded organic soil, which meets the IPCC definition of “organic soil”. We test two hypotheses: firstly, GHG emissions (mainly CO₂) of histic Gleysols increase linearly with drainage depth in the peat layer and level off when the water table falls below the peat layer. Secondly, peat mixed with mineral subsoil and resulting lower C_{org} concentration emits lower amounts of GHG than unmixed peaty soil with a high C_{org} concentration.

2 Material and methods

2.1 Study site Grosses Moor [Great Peat Bog]

The Grosses Moor [Great Peat Bog] (Gifhorn, Germany; 52°34′54.22″ N, 10°39′46.43″ E) is a bog-fen peat complex of 6000 hectares situated close to the eastern climatic boundary for bog formation. It is located within a former moraine plain from the Saale ice age and the meltwater of the Warthe stage initiated bog formation (Overbeck, 1952). The original

ombrotrophic peat bog was altered by peat drainage and peat cutting during the 19th century. As a result, nowadays the Grosses Moor is influenced by groundwater. Mean annual temperature was 8.5 °C and mean annual precipitation was 663 mm in the time period 2008–2011. Mineral substrates below the peat are sandy terraces and partly Pleistocene clay layers. Formerly up to six metre deep peat layers were altered by peat cutting and deep plough cultivation, which created strong small-scale heterogeneity. The original bog vegetation has been nearly completely destroyed. Typical vegetation now consists of large cultivated areas, grasslands, and forests of pine and birch as well as purple moor-grass (*Molinia caerulea*), soft rush (*Juncus effusus*) and Erica heath in peat harvest areas. About 2700 hectares were turned into restoration areas in 1984. About 2720 hectares of abandoned peat cut areas are used as extensive grassland.

The study area is managed as extensive grassland. Sheep graze one to three times a year. Mulching is conducted in autumn. No fertilizer is applied.

The study area is characterized by small peat shoulders and depressions with different water table levels and an irregular anthropogenic mixing of peat layer and mineral soil. Although the entire study area is classified as grassland, the vegetation also shows a gradient from grass dominance to moss dominance.

The small-scale heterogeneity of the study area was surveyed to select sites with diverging soil organic carbon (SOC) concentration in topsoil, C stocks, and water table levels. According to a survey report and own preliminary investigations, two transects (each 310 m) were established at 100 m distance from each other in the area of the field where peat cutting and sand mixing from ploughing into strata beneath the peat layer occurred. Every ten metres sampling was carried out by auger until the sandy layer was reached. Auger samples were divided into 0–0.3 m (peat layer) and 0.3–0.6 m (sandy layer). For a first assessment, indicative levels of the carbon content of the peat layer were determined by loss on ignition. Six sites were selected in order to achieve similar peat depths (0.25–0.3 m), differing SOC concentrations, and differing water levels. The resulting site characteristics are presented in Table 1. Sites with a C_{org} content below 15 % were classified as C_{low}, > 15 % to 35 % C_{org} as C_{med}, and > 35 % to 55 % C_{org} as C_{high}. Mean groundwater levels *W* during the study period are indicated by index in centimetres below soil surface. As a result, sites C_{med} W₃₉, C_{low} W₂₉ and C_{low} W₁₄ are located on transect 1 within 70 m distance and sites C_{high} W₁₁, C_{high} W₂₂ and C_{high} W₁₇ on transect 2 within 30 m distance. Sites were fenced to keep off sheep and other animals.

2.2 Measurement of site characteristics

Photosynthetic active radiation (PAR), precipitation, and air temperature were continually measured at a local meteorological station which was located at a distance of 100 to

Table 1. Site characterization.

Site ^a	Soil class (WRB)	C _{org} [%] ^b	C stock [kg m ⁻²] ^b	bulk density [g cm ⁻³] ^b	C/N ^b	N _{min} [kg ha ⁻¹] ^c	pH (CaCl ₂)	Mean GWL [m] ^d
C _{med} W ₃₉	histic Gleysol	34.3	46	0.54	29	6 ± 3	3.8	0.39
C _{low} W ₂₉	mollic Gleysol	11.3	36	1.06	27	17 ± 11	4.5	0.29
C _{low} W ₁₄	mollic Gleysol	9.3	29	0.97	24	10 ± 5	4.5	0.14
C _{high} W ₁₁	histic Gleysol	51.7	71	0.45	28	2 ± 1	4.1	0.11
C _{high} W ₂₂	histic Gleysol	47.7	41	0.29	28	2 ± 1	3.8	0.22
C _{high} W ₁₇	histic Gleysol	47.7	41	0.29	28	2 ± 1	3.8	0.17

C = carbon, W = mean annual water table. ^a Subscripts in site designations refer to low (< 15 %), medium (15–35 %) or high (> 35 %) soil C content and mean annual water table depth (cm). ^b Organic carbon, C stock, C/N and bulk density in 0–30 cm. ^c Site mean value ± one standard deviation of mineral nitrogen in 0–20 cm in the time interval 1 June 2011 to 1 June 2012 ($n = 27$). ^d GWL = ground water level in the time interval 1 June 2011 to 1 June 2012.

150 m from the sites. PAR was manually logged at each site during measurements.

Groundwater levels were continually recorded at each site every 15 min by groundwater data loggers (Mini-diver, Schlumberger). In order to eliminate short-term disturbances, a moving median was calculated over a 75 min window. Subsequently, moving median values were aggregated to one-hour values.

Soil temperatures in 0.1, 0.05, and 0.02 m were continually logged at each site every 5 min by soil temperature sensors.

Mineral nitrogen (N_{min}) contents of the 0–0.2 m soil layer were analysed according to VDLUFA (1997) by extraction with 0.01 M CaCl₂ at every N₂O measurement. For each site the measured N_{min} values were extrapolated to N_{min} stocks per hectare. The pH values were determined with CaCl₂ according to DIN ISO 10390 (HBU, 2005). C_{org} of each site was measured with an elemental analyser (variomax C, Elementar). Bulk density was measured according to DIN ISO 11272 in 0–0.3 m (HBU, 1998).

Plant species were determined according to Oberdorfer (2001) and species abundance was classified according to the Londo scale (Londo, 1976). Sedge, grass and moss cover was determined for every site.

Green biomass was manually harvested from the plots after each grazing by cutting to 5 cm above the soil surface. At all sites only the grass and sedge biomass was removed; mosses were left untouched. Fresh weight and weight after drying at 60 °C were determined. For carbon and nitrogen measurement (Leco, TruMac CN) a pooled and homogenized sample of all biomass from a plot was used. The C and N values of three replicate plots were averaged per site. C and N contents of the biomass of all cut dates were summed and defined as the biomass export of each site.

2.3 GHG flux measurements

CO₂, CH₄, and N₂O fluxes were measured with manual static chambers (Drösler, 2005) at the six sites. Rows of triplicate chamber frames (0.61 m², 0.4 m distance between frames) were installed on each site for gas flux measurements. Measurements were conducted at least fortnightly. For CO₂, three sites were measured per day, i.e. C_{med} W₃₉, C_{low} W₂₉ and C_{low} W₁₄ on one day and C_{high} W₁₁, C_{high} W₂₂ and C_{high} W₁₇ on another day.

Diurnal cycles of CO₂ fluxes covering the full range of PAR and soil temperature of a day were measured from sunrise till late afternoon with an infrared gas analyser (LI-820, LI-COR, USA) connected to opaque PVC chambers (for ecosystem respiration, chamber height 0.5 m, 2 to 5 min chamber closure) and transparent plexiglass chambers (for net ecosystem exchange, chamber height 0.5 m, 1.5 to 3 min chamber closure) (PS-plastic, Eching, Germany). Exclusion criteria of CO₂ fluxes were PAR changes larger than 10 % of the starting value and more than 1.5 °C increase in chamber temperature. However, few fluxes were removed ex post from the data set due to these criteria, since they could be checked in the field and measurements were adjusted accordingly. For cooling of the transparent chambers thermal packs were used. During each campaign each frame was sampled by opaque chambers three to six times and by transparent chambers five to eight times depending on season and weather conditions.

Opaque PVC chambers were used for CH₄ and N₂O flux measurements (PS-plastic, Eching, Germany). Chamber air samples were collected in headspace vials 0, 20, 40, and 60 min after chamber closure. Measurements were carried out with a Varian CP-3800 GC-FID/-ECD using a headspace autosampler (QUMA Elektronik & Analytik GmbH, Germany).

The period used for carbon and GHG annual balance was chosen from 1 June 2011 until 1 June 2012.

2.4 CO₂ modeling

2.4.1 Raw fluxes

Fluxes were calculated by linear regression with CO₂-Flux Version 1.0.30 (Beetz et al., 2013). Near zero fluxes with small R^2 were not discarded (Alm et al., 2007). A 50-point moving window (measurement frequency 1.3 s) was applied to find fluxes with maximum R^2 and minimum variance, respectively. Both optimization procedures resulted often in identical flux estimates (53 % of all fluxes), but differed in particular during sunrise. Therefore, the mean value of the fluxes from the two optimization procedures was used as a somewhat conservative flux estimate. 19 % of all fluxes had a difference of less than 5 % between the two procedures and 14 % of all fluxes had a difference of more than 20 %. Daily net ecosystem exchange (NEE), ecosystem respiration (R_{eco}), and gross primary production (GPP) were modelled according to Alm et al. (1997), Drösler (2005), and Beetz et al. (2013) with some adaptations to site conditions as described below.

2.4.2 Response functions

Since the transparent chambers absorb a maximum of five percent of the incoming radiation according to the manufacturer (PS-plastic, Echting, Germany), the PAR data from the measurement campaigns were corrected by a factor of 0.95. Diurnal cycles of PAR values differed between on-site measurements and measurements at the meteorological station. This was corrected using empirical functions ($\text{PAR} = a \times \text{PAR}_{\text{station}}^b$), which were derived separately for sites C_{med} W_{39} , C_{low} W_{29} and C_{low} W_{14} and sites C_{high} W_{11} , C_{high} W_{22} and C_{high} W_{17} , respectively, using robust non-linear regression (Rousseeuw et al., 2012; Fig. S1 in the Supplement). The location of the sites and the meteorological station were at different distances from an adjacent tree line, which resulted in different times when direct sunlight reached the PAR sensors at dawn. Since the meteorological station logged every 0.5 h, but the radiation conditions changed at a higher frequency, additional scatter occurred in the data due to clouds and other effects.

The temperature-dependent R_{eco} flux model was calculated according to Lloyd and Taylor (1994):

$$R_{\text{eco}} = R_{\text{ref}} \times \exp \left[E_0 \times \left(\frac{1}{T_{\text{ref}} - T_0} - \frac{1}{T - T_0} \right) \right]. \quad (1)$$

R_{ref} respiration at the reference temperature [$\text{mg CO}_2\text{-C m}^{-2} \text{h}^{-1}$]; E_0 an activation-like parameter [K]; T_{ref} reference temperature: 283.15 [K]; T_0 temperature constant for the start of biological processes: 227.13 [K].

The model was fitted to soil temperatures in 0.02 m depth, which resulted in robust fits (see Fig. S3 in the Supplement)

and was considered to be representative both of plant and of soil respiration. On-site temperatures were used for fitting rather than temperatures from the meteorological station as they resulted in better fit quality. If fitting the temperature dependence was numerically not possible, e.g. due to the observed temperature range during a measurement campaign being too narrow, the campaign was excluded from calibration and only used for validation (Fig. S4 in the Supplement). This was applied to two winter campaigns (1 °C temperature range in 2 cm). The temperature ranges were campaign dependent with an average range of 5 to 13 °C in 2 cm. The R_{eco} models of the measurement campaigns had a median R^2 of 0.98 and a minimum of 0.83.

The PAR-dependent NEE flux model was calculated using the Michaelis–Menten type model proposed by Falge et al. (2001) (see Fig. S3 in the Supplement):

$$\text{NEE} = \frac{(\text{GP2000} \times \alpha \times \text{PAR})}{\left(\text{GP2000} + \alpha \times \text{PAR} - \frac{\text{GP2000}}{2000} \times \text{PAR} \right)} + R_{\text{eco}}. \quad (2)$$

GP2000 rate of carbon fixation at PAR 2000 [$\text{mg CO}_2\text{-C m}^{-2} \text{h}^{-1}$]; PAR photon flux density of the photosynthetic active radiation [W m^{-2}]; α initial slope of the curve; light use efficiency [$\text{mg CO}_2\text{-C m}^{-2} \text{h}^{-1} / \text{W m}^{-2}$].

The NEE models of the measurement campaigns had a median R^2 of 0.97 and a minimum of 0.60.

PAR values used for fitting were again on-site values.

2.4.3 Interpolation to annual models

The annual model was calculated separately for each site. Values between two measurement campaigns were calculated separately using the campaign results on both sides, and then taken as the distance weighted mean of both values. To account for management events, E_0 and R_{ref} were kept constant from the preceding measurement campaign until the cut date. After the cut parameters were taken from the subsequent measurement campaign. The annual R_{eco} model was calculated on a 0.5 hourly basis using on-site temperature data. Biomass cuts were included in the NEE model by applying α and GP2000 from the preceding measurement campaign until the cut date and setting α to -0.01 and GP2000 to -4 after the cut according to observations on other grassland sites (Drösler et al., 2013). NEE values were modelled using corrected PAR values from the meteorological station. In the end GPP was calculated on a 0.5 hourly basis:

$$\text{GPP} = \text{NEE} - R_{\text{eco}}. \quad (3)$$

For error estimation of the CO₂ fluxes (NEE, GPP, R_{eco}) and to construct a confidence interval for the annual NEE, GPP and R_{eco} fluxes, a Monte Carlo simulation was conducted for each site as follows:

1. The robust fit of the PAR correction function was performed 1000 times with bootstrap resamples of the PAR data points (on-site/station).

2. From the R_{eco} fits of all measurement campaigns bootstrap parameter samples were created using bootstrap of the residuals (Efron, 1979). Bootstrap of the residuals preserves the distribution of x values, which is particularly important for small data size. The bootstrap sample size was again 1000, but bootstrap fits were discarded if they did not successfully model a temperature dependence ($E_0 = 0$). On average 70 % of the fits were successful. Using these, about 700 annual R_{eco} models were calculated for each site. The medians of these models were in excellent agreement with the original models. 97.5 % and 2.5 % quantiles at each time point were used to construct confidence intervals of the time series. Confidence intervals of the annual sums were constructed in the same way.
3. Each R_{eco} bootstrap fit was paired with a PAR correction bootstrap fit and based on these the NEE models were refitted for each site and measurement campaign. With these NEE fits, bootstrap of the residuals was conducted as described above. Again only successful fits (52 % on average) were used. The high number of failed fits results from the strong non-linearity of the NEE model and the relatively low number of data points at each measurement campaign. About 364 000 (700×520) annual models were calculated from the bootstrap parameter samples and confidence intervals constructed as described before.

2.5 CH₄ and N₂O flux calculation

The following algorithm was used to calculate CH₄ and N₂O fluxes:

1. Flux rates were calculated using ordinary linear regression, robust linear regression (Huber, 1981), and Hutchinson–Mosier regression (HMR; Pedersen et al., 2010).
2. For the standard case of 4 data points the flux calculated by robust linear regression was used per default. Only if the following conditions were met, was the non-linear flux estimation (HMR) used instead:
 - a. the HMR function could be fitted,
 - b. Akaike information criterion (AIC; Burnham and Anderson, 2004) was smaller for HMR fit than for linear fit,
 - c. p value of flux calculated using HMR was smaller than that from robust linear fit,
 - d. and the flux calculated using HMR was not more than 4 times the flux from robust linear regression. This avoided severe overestimation of fluxes (see Fig. S5 for an example).

3. Ordinary linear regression was applied for three data points. If less than three data points were available (due to loss of samples) no flux was calculated and the measurement discarded.

As a result, 27 % of all CH₄ fluxes and 16 % of all N₂O fluxes were calculated non-linearly. Depicting square roots of the flux standard error (calculated from the regressions) in box-plots and histograms showed distributions relatively similar to normal distribution. Median standard errors were $12 \mu\text{g CH}_4\text{-C m}^{-2} \text{h}^{-1}$ and $3 \mu\text{g N}_2\text{O-N m}^{-2} \text{h}^{-1}$, which demonstrates a good accuracy of the flux measurements. Some extreme standard error values were detected. Associated flux values were considered carefully as potential outliers based on field and lab notes as well as the pattern of CO₂ concentrations. If the third or last CO₂ concentration was not plausible, e.g. lower than the previous one, the sample was deleted and linear regression applied. If an outlier occurred with CH₄ and N₂O fluxes and not with CO₂, values were not corrected since CH₄ and N₂O were often near ambient or near zero fluxes occurred.

Mean annual fluxes were calculated by linear interpolation between measurement campaigns.

2.6 Statistical analyses

R 2.15.2 (R Core Team, 2012) was used for statistics and modelling. In particular, package *nlme* (package version 3.1.108; Pinheiro et al., 2013) was used for linear mixed-effects models.

3 Results

3.1 Driver variables

In the investigation period, daily mean value of the air temperature ranged from -14.8 to 23.5 °C and the 0.02 m soil temperatures were between -1.6 °C and 20.7 °C. Daily mean air temperature was below zero degrees Celsius on 27 days, while this was the case for soil temperature on 11 days (Fig. 1). A longer period of snow cover occurred during February 2012.

Groundwater levels (GWL) were within the peat layer at each site during different periods. At the driest sites ($C_{\text{med}} W_{39}$ and $C_{\text{low}} W_{29}$) GWLs were in the peat layer for 128 and 214 days, respectively. In contrast, sites $C_{\text{low}} W_{14}$, $C_{\text{high}} W_{22}$ and $C_{\text{high}} W_{17}$ had a similar number of days with high water levels (304, 271 and 273, respectively), whereas at the wettest site ($C_{\text{high}} W_{11}$) water levels were within the peat layer for the whole year. Groundwater levels above the surface occurred only on the wet sites ($C_{\text{low}} W_{14}$, $C_{\text{high}} W_{11}$, and $C_{\text{high}} W_{17}$) during 83, 34, and 35 days, respectively. Longer periods of water saturation were observed on these sites during the winter season, whereas during the summer season few precipitation events caused short periods of flooding. Site

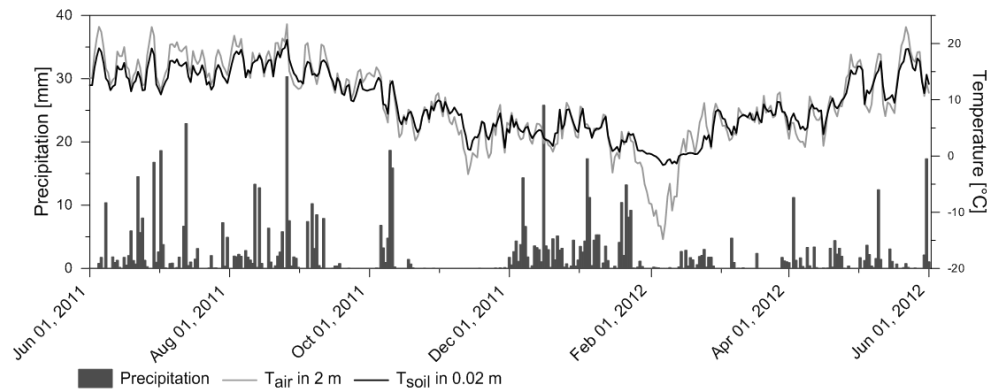


Fig. 1. Time series of precipitation, air, and 2 cm soil temperature at the meteorological station.

$C_{\text{high}} W_{11}$ showed the lowest groundwater level dynamics, whereas site $C_{\text{med}} W_{39}$ had the highest groundwater level dynamics of all sites (Fig. S2 in the Supplement).

Mineral nitrogen stock was low at all sites (Table 1). The maximum value of 17 kg ha^{-1} was found at site $C_{\text{low}} W_{29}$ with the highest plant biomass, whereas the moss-dominated sites $C_{\text{high}} W_{11}$, $C_{\text{high}} W_{22}$ and $C_{\text{high}} W_{17}$ contained the smallest N_{min} stocks of 2 kg ha^{-1} . The N_{min} differences between the sites were also reflected in vegetation composition and biomass amounts.

Plant species composition and vegetation cover were similar within one site, whereas vegetation showed clear differences between the individual sites (Table 2). Sites where the histic horizon was mixed with sand, or the mean annual water table was below about 20 cm, had high abundance of grasses and moderate productivity. Sphagnum and other mosses were present on sites with high C_{org} and little drainage, where productivity was low. In detail, $C_{\text{med}} W_{39}$, $C_{\text{low}} W_{29}$ and $C_{\text{low}} W_{14}$ were dominated by sedges and grasses in different levels and without any moss occurrence, which is also reflected in the highest biomass exports (1.7 to $2.9 \text{ t ha}^{-1} \text{ a}^{-1}$; three grazing events and one mulching event) in comparison with the other sites. In contrast, $C_{\text{high}} W_{11}$, $C_{\text{high}} W_{22}$ and $C_{\text{high}} W_{17}$ had high moss abundance and a lower grass and sedge biomass. The biomass export on these sites was only in the range of 0.3 to $0.6 \text{ t ha}^{-1} \text{ a}^{-1}$ during one grazing and one mulching event.

3.2 CO₂

Gross primary production on sites $C_{\text{med}} W_{39}$, $C_{\text{low}} W_{29}$ and $C_{\text{low}} W_{14}$ was about $12 \text{ t C ha}^{-1} \text{ a}^{-1}$, whereas on sites $C_{\text{high}} W_{11}$, $C_{\text{high}} W_{22}$ and $C_{\text{high}} W_{17}$ GPP was about $6 \text{ t C ha}^{-1} \text{ a}^{-1}$ (Table 3), reflecting the difference in biomass productivity and nitrogen content between the different sites (Tables 1 and 2).

During the vegetation period plant growth influenced NEE budgets of all sites, which as a result became CO₂ sinks as well as CO₂ sources over the course of the year (especially right after grazing). From October until March NEE fluxes were at a low level on all sites and they were dominated by R_{eco} since GPP was near zero on all sites (Fig. 2).

$C_{\text{med}} W_{39}$, $C_{\text{low}} W_{29}$ and $C_{\text{low}} W_{14}$ showed a similar time series (Fig. 2). However, in spring and summer GPP gradually decreased from $C_{\text{low}} W_{29}$ to $C_{\text{med}} W_{39}$ and $C_{\text{low}} W_{14}$. This is in line with the productivity differences of grass and sedge species on the respective sites. $C_{\text{high}} W_{11}$, $C_{\text{high}} W_{22}$ and $C_{\text{high}} W_{17}$ also feature similar time series. Although in spring and summer the GPP of site $C_{\text{high}} W_{22}$ was larger than on sites $C_{\text{high}} W_{17}$ and $C_{\text{high}} W_{11}$, these three sites had nearly identical annual GPP fluxes. GPP is in line with the different productivity of grass and sedge vs. moss species (Table 2).

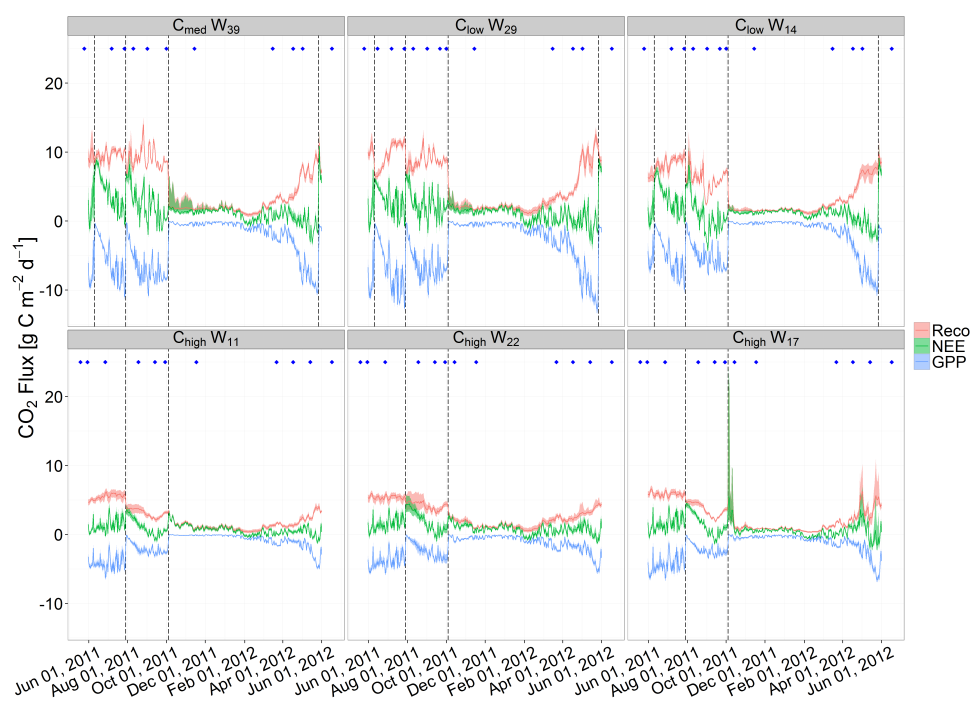
Ecosystem respiration of sites $C_{\text{med}} W_{39}$, $C_{\text{low}} W_{29}$ and $C_{\text{low}} W_{14}$ (about $18 \text{ t C ha}^{-1} \text{ a}^{-1}$) was nearly twice as high as of sites $C_{\text{high}} W_{11}$, $C_{\text{high}} W_{22}$ and $C_{\text{high}} W_{17}$ ($10 \text{ t C ha}^{-1} \text{ a}^{-1}$). This again reflects the vegetation differences. The same trends were found between the sites as before for GPP. This leads to the assumption that plant respiration was dominating R_{eco} differences between the sites, which is confirmed by highly significant correlations between daily mean values of GPP and R_{eco} for each site ($p < 2.2 \times 10^{-16}$, mean R^2 0.64 for all sites).

All of the sites in the Grosses Moor were both source and sink of CO₂ at different times, with some clear annual NEE trends (Fig. 2). $C_{\text{med}} W_{39}$, $C_{\text{low}} W_{29}$ and $C_{\text{low}} W_{14}$ exhibited NEE values of about $5 \text{ t C ha}^{-1} \text{ a}^{-1}$, whereas sites $C_{\text{high}} W_{11}$ and $C_{\text{high}} W_{17}$ had an NEE of about $3 \text{ t C ha}^{-1} \text{ a}^{-1}$ only (Table 3). NEE of site $C_{\text{high}} W_{22}$ was between the two groups. Differences between sites in annual NEE were less prominent than for GPP and R_{eco} . Grass-dominated sites, the sites with higher plant productivity, exhibited higher NEE fluxes than sites containing predominantly mosses. However, low

Table 2. Biomass export from sites (1 June 2011 to 1 June 2012; site mean value \pm one standard deviation between replicate plots) and cover of sedges, grasses and mosses.

Site ^a	Mg C ha ⁻¹ a ⁻¹	kg N ha ⁻¹ a ⁻¹	sedge cover [%] ^b	grass cover [%] ^b	moss cover [%] ^b
C _{med} W ₃₉	2.26 \pm 0.10	95 \pm 3	10	70	0
C _{low} W ₂₉	2.92 \pm 0.14	138 \pm 7	0	90	0
C _{low} W ₁₄	1.69 \pm 0.28	68 \pm 10	55	15	0
C _{high} W ₁₁	0.28 \pm 0.03	8 \pm 1	35	25	95
C _{high} W ₂₂	0.57 \pm 0.04	19 \pm 2	15	65	65
C _{high} W ₁₇	0.39 \pm 0.02	14 \pm 1	50	20	75

^a Subscripts in site designations refer to low (< 15 %), medium (15–35 %) or high (> 35 %) soil C content and mean annual water table depth (cm). ^b Cover values are indicated nearest to 5 %. Since the cover of grasses, sedges and mosses is observed separately and species can overlap, the total plot cover can exceed 100 %.

**Fig. 2.** Time series of daily CO₂ fluxes [g C m⁻² d⁻¹] at each site (1 June 2011–1 June 2012). Depicted are modelled fluxes and 95 % confidence band. Dashed lines indicate grazing and mulching events. Diamonds indicate measurement campaigns.

NEE fluxes occurred on all sites during the winter season because grasses were cut in autumn.

3.3 CH₄

CH₄ fluxes were at a low level, with the highest CH₄ emissions at site C_{high} W₁₇, whereas site C_{low} W₂₉ emitted the lowest amounts of CH₄ (Table 3), reflecting water level differences. Annual fluxes ranged from 3 to 203 kg C ha⁻¹ a⁻¹ and therefore all sites represented small sources.

Strongest CH₄ emissions occurred during periods with high water levels and warm temperatures (Fig. S6a in the Supplement).

3.4 N₂O

Only near zero N₂O fluxes and no emission peaks occurred at any site. Annual fluxes ranged from 0.5 kg N₂O–N ha⁻¹ a⁻¹ to 1.4 kg N₂O–N ha⁻¹ a⁻¹ and were not significant ($p > 0.05$ according to a t test with Bonferroni adjustment for multiple testing; Fig. S6b in the Supplement).

Table 3. Annual fluxes of NEE, Reco and GPP, CH₄ and N₂O (1 June 2011 to 1 June 2012; annual flux ± uncertainty^a).

Site ^b	NEE [Mg C ha ⁻¹ a ⁻¹]	Reco [Mg C ha ⁻¹ a ⁻¹]	GPP [Mg C ha ⁻¹ a ⁻¹]	CH ₄ [Mg C ha ⁻¹ a ⁻¹]	N ₂ O [kg N ha ⁻¹ a ⁻¹]
C _{med} W ₃₉	6.3 ± 0.4	18.6 ± 0.4	-12.3 ± 0.2	0.003 ± 0.003	1.09 ± 0.17
C _{low} W ₂₉	5.7 ± 0.4	19.7 ± 0.4	-14.0 ± 0.3	-0.003 ± 0.003	1.40 ± 0.23
C _{low} W ₁₄	4.9 ± 0.3	15.4 ± 0.3	-10.5 ± 0.2	0.104 ± 0.030	0.98 ± 0.16
C _{high} W ₁₁	3.0 ± 0.3	8.6 ± 0.3	-5.6 ± 0.2	0.203 ± 0.067	0.51 ± 0.15
C _{high} W ₂₂	3.9 ± 0.3	10.4 ± 0.3	-6.5 ± 0.2	0.021 ± 0.009	0.50 ± 0.36
C _{high} W ₁₇	3.2 ± 0.4	9.6 ± 0.3	-6.5 ± 0.2	0.141 ± 0.037	0.66 ± 0.11

^a Uncertainty values represent the accumulated measurement uncertainty and spatial heterogeneity, given for NEE, Reco and GPP as ± one standard deviation calculated by the Monte Carlo method, and for CH₄ and N₂O as ± one standard deviation of the replicates. ^b Subscripts in site designations refer to low (< 15%), medium (15–35%) or high (> 35%) soil C content and mean annual water table depth (cm).

3.5 Annual C and GHG balance

Including the carbon from vegetation export (Table 2) and from CH₄ emissions (Table 3), the annual carbon balance of the sites was in the range of 3.5 to 8.8 t C ha⁻¹ a⁻¹ (Table 4, GWP-GHG balance).

Differences in the amount of exported carbon altered the ranking of sites according to their annual carbon and greenhouse gas balance compared with their NEE ranking. Sites C_{low} W₂₉ and C_{med} W₃₉ emitted more GHGs than site C_{low} W₁₄. This indicates that higher productive sites emitted more GHGs. More distinct differences between the sites became apparent this way than if NEE was considered in isolation. The ranking of the sites according to their GHG balance did not change if N₂O emissions were included (Table 4).

4 Discussion

4.1 Magnitude of GHG fluxes

The CO₂ fluxes of the Grosses Moor are within the range of other studies in comparable German peatlands (e.g. Drösler, 2005) as well as in peatlands of northern latitudes (e.g. Alm et al., 1997; Bellisario et al., 1998). Similar NEE fluxes and biomass export were observed on drained permanent grassland in Denmark (Elsgaard et al., 2012). In comparison with further German grassland sites on organic soils, emissions of the Grosses Moor are in the upper range of all considered GHG balances (Fig. 3; Drösler et al., 2013).

Low CH₄ emissions similar to those from the dry sites (C_{med} W₃₉ and C_{low} W₂₉) were reported by Drösler (2005) for a dry, peat cut heath. The two sites with the highest fluxes (C_{high} W₁₁ and C_{high} W₁₇) are in the lower third of average emission rates of 5–80 mg CH₄-C m⁻² d⁻¹ given by Blodau (2002) for natural peatlands. Comparable low CH₄ fluxes were found in three drained Danish peatlands, increasing with higher cover of plants with aerenchymatic tissues (Schäfer et al., 2012). Also in the Grosses Moor, sites with a higher cover of sedges (Table 3) emitted more CH₄. Because of their aerenchymatic tissue, which channels CH₄

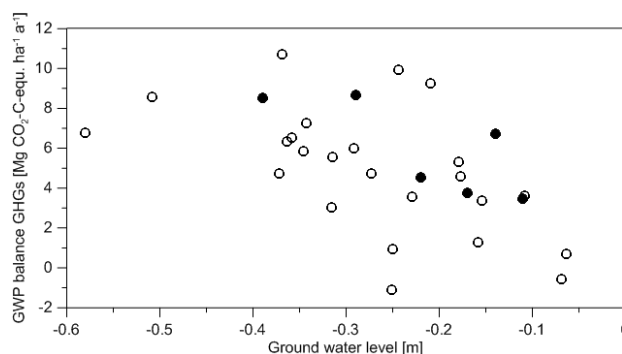


Fig. 3. Annual GHG balances vs. water table level of shallow peat sites in the Grosses Moor (filled circles) and several deep peat grassland sites (open circles) in Germany (Drösler et al., 2013).

fluxes from soil, sedges prevent CH₄ from further oxidation by soil microbes (Thomas et al., 1996). Low water levels during warm periods can result in oxidation of CH₄ by methanotrophic bacteria to CO₂ in the aerated soil zone, thereby increasing respiration (Lai, 2009). According to Blodau (2002) large root density can increase CH₄ oxidation, which results in low CH₄ emission rates at the soil surface. The CH₄ emission patterns observed at the Grosses Moor are in accordance with these mechanisms.

Low N₂O values as in the Grosses Moor were reported for a dry peat cutting area by Drösler (2005). In soils with C/N ratios above 25 (Table 1), low N₂O emissions can be expected (Klemmedtsson et al., 2005). Other drained peatlands with permanent grass cover but deeper peat layers emitted even lower amounts of N₂O (Petersen et al., 2012). The Grosses Moor reacts like nutrient-poor bogs with regard to N₂O.

4.2 Precision of the annual CO₂ budget

Our error analysis is based in principle on the bootstrap approach and error propagation using Monte Carlo simulation. Resulting confidence intervals, which include measurement error as well as on-site heterogeneity, were overall relatively

Table 4. Global warming potential for a time horizon of 100 yr (GWP100) of Net C balance (NEE plus harvest), CH₄ and N₂O and total GHG balance (annual flux \pm uncertainty^a; Forster et al., 2007).

Site ^b	GWP100-C balance [Mg CO ₂ -C eq ha ⁻¹ a ⁻¹]	GWP100-CH ₄ [Mg CO ₂ -C eq ha ⁻¹ a ⁻¹]	GWP100-N ₂ O [Mg CO ₂ -C eq ha ⁻¹ a ⁻¹]	GWP100-GHG balance [Mg CO ₂ -C eq ha ⁻¹ a ⁻¹]
C _{med} W ₃₉	8.5 \pm 0.4	0.003 \pm 0.003	0.146 \pm 0.023	8.7 \pm 0.4
C _{low} W ₂₉	8.6 \pm 0.4	-0.003 \pm 0.003	0.188 \pm 0.030	8.8 \pm 0.4
C _{low} W ₁₄	6.6 \pm 0.4	0.104 \pm 0.030	0.131 \pm 0.021	6.8 \pm 0.4
C _{high} W ₁₁	3.3 \pm 0.3	0.203 \pm 0.067	0.068 \pm 0.020	3.5 \pm 0.3
C _{high} W ₂₂	4.5 \pm 0.3	0.021 \pm 0.009	0.067 \pm 0.049	4.6 \pm 0.3
C _{high} W ₁₇	3.5 \pm 0.4	0.141 \pm 0.037	0.088 \pm 0.015	3.8 \pm 0.4

^a Uncertainty values represent the accumulated measurement uncertainty and spatial heterogeneity, given for GWP 100-C as \pm one standard deviation calculated by the Monte Carlo method, and for CH₄ and N₂O as \pm one standard deviation of the replicates. Uncertainty values of the GHG balance were derived using Gaussian error propagation. ^b Subscripts in site designations refer to low (< 15 %), medium (15–35 %) or high (> 35 %) soil C content and mean annual water table depth (cm).

narrow (Fig. 2). However, the interpolation between the measurement campaigns could constitute a significant additional source of error. The calibration of temperature and PAR models by frequent campaigns captures effects of changing water table and biomass, but for interpolation between campaigns we assume a linear change from one calibration to the next one. With the available data it was not possible to quantify the interpolation error in the error analysis. The interpolation error could be quantified by very frequent measurement campaigns with automated chambers. We used measurement campaigns, which did not result in adequate model fits, to validate the interpolation. The CO₂ fluxes of the validation campaigns were well described by the models, so that we can conclude that the interpolation is relatively robust (Fig. S4 in the Supplement).

Most of the CO₂ measurement campaigns covered the full range of temperature and radiation for the interpolation, so that the model error remained low for most of the time and the method was robustly applied. There were few periods (< 5 days in summer and < 47 days in winter) for which temperature was continuously outside the temperature range of at least one of the adjacent campaign days. These periods are characterized by higher model uncertainty due to extrapolation of the R_{eco} fits (Fig. 2).

Our NEE error estimates (about ± 0.4 Mg C ha⁻¹ yr⁻¹) without interpolation error were at the low end of error estimates for eddy covariance measurements, for which errors in the range of ± 0.3 to ± 1.8 Mg C ha⁻¹ yr⁻¹ (Woodward and Lomas, 2004) or higher (Kruijt et al., 2004) have been reported. We expect that the error of the chamber-based approach with interpolation error is likely to be comparable with eddy covariance. Thus, the chamber technique with model-based CO₂ flux interpolation is a reliable method for studying small-scale heterogeneity and sites where eddy covariance is not applicable.

4.3 C_{org} effects

The GHG fluxes of the histic grasslands of the Grosses Moor are in the upper range of German managed grassland sites on organic soils with deep peat layers (Fig. 3; Drösler et al., 2013). This is opposite to our expectation of lower GHG emissions from soil with shallow histic layers, in which less soil organic carbon is exposed to mineralization by drainage than in soils with deep peat layers. Obviously, the substrate quality and decomposition level of the peat play a larger role in emission rates (Berglund and Berglund, 2011) than peat depth. Our results are in accordance with Reiche et al. (2010), who did not find a clear relationship for the prediction of CO₂ and CH₄ production rates under anoxic conditions in dependence on the degree of humification.

We defined the effective C stock as the fraction of aerated carbon in the soil profile. Effective C stock showed no effect on GHG emissions. Moreover, no significant correlation was found between C_{org} concentration in the topsoil and GHG emissions (Fig. 4a).

All sites exhibited highly degraded (H10 on the Van-Post scale; AG Boden, 2005), amorphous organic material in the peat layer (0 to 0.3 m). The sand intermixture (C_{med} W₃₉, C_{low} W₂₉ and C_{low} W₁₄) resulted in yield increase via harvested biomass (Table 2) instead of C_{org} stabilization on the mineral phase. We therefore reject our hypothesis that peat mixed with mineral subsoil and resulting lower C_{org} concentration emits lower amounts of GHG than unmixed peat soil with a high C_{org} concentration.

Mixing peat with sand has been a widespread soil management practice to improve the suitability of peat soils for agriculture (Göttlich, 1990) and is still practiced today. Our findings suggest that peat mixing does not mitigate GHG emissions from high organic carbon soils.

This finding has serious consequences for regional to national GHG balances because histic Gleysols are relatively widespread. Due to a lack of data, shallow or mixed organic soils such as histic Gleysols, which do not fall under the definition of Histosols but do fall under the definition of organic

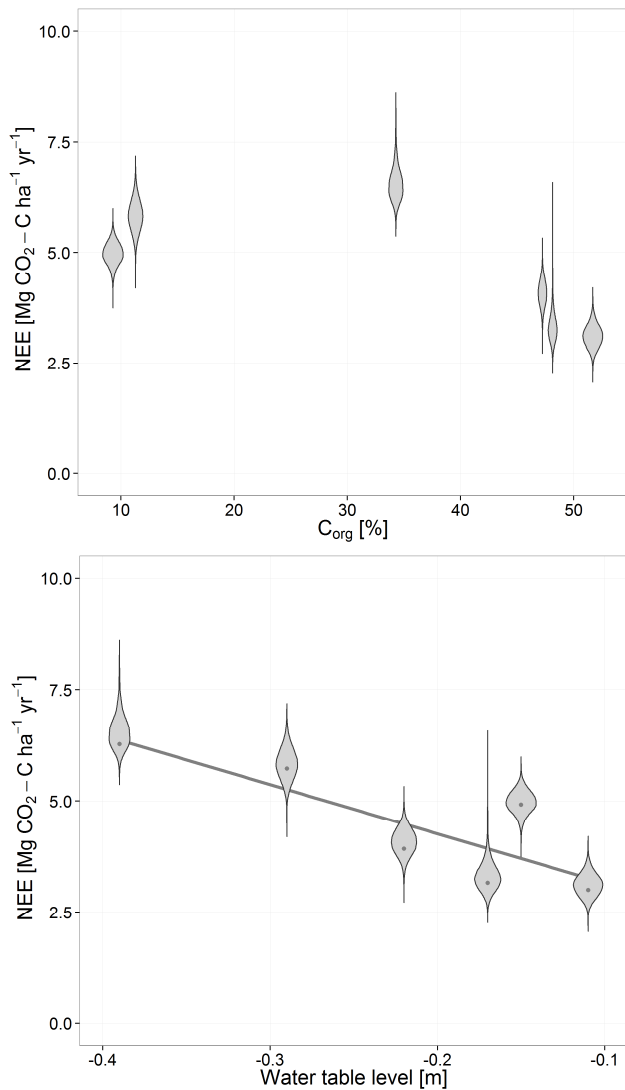


Fig. 4. Violin plots of NEE emissions vs. C_{org} (A; $R^2 = 0.49$, $p = 0.121$) and NEE emissions vs. water table level (B; $R^2 = 0.71$, $p = 0.035$). Violins (A, B): distribution of all simulated aggregated annual NEE sums of each site; points (B): modelled annual NEE of each site, used as basis for linear regression.

soils of the IPCC (IPCC, 2006), tended to be neglected as a source of GHGs in national GHG inventories under the UNFCCC or estimated to emit half of the annual CO₂ emissions of real Histosols (Nielsen et al., 2012). Adding histic Gleysols to the Histosol area, the land area with GHG emission hotspots due to drainage is likely to be much larger than anticipated.

4.4 Water level effects

The variation between measurement campaigns showed that GPP was not significantly influenced by water levels but

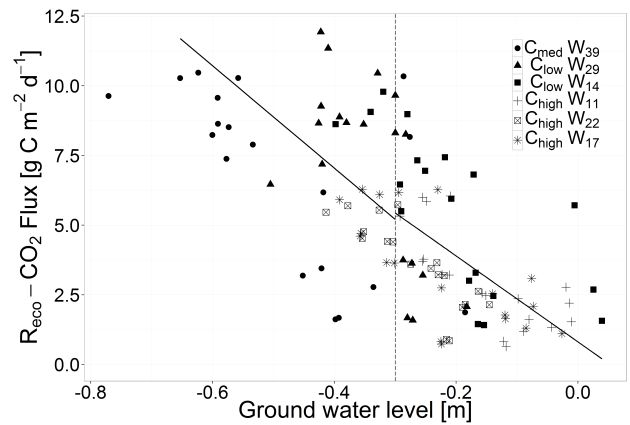


Fig. 5. Ground water levels [m] vs. $R_{\text{eco}}\text{-CO}_2$ Flux [g C m⁻² d⁻¹] on the campaign dates for all six sites. Dotted vertical line: border of peat horizon; continuous line: population mean prediction from the linear mixed effects model for all sites; a fixed effect was used to distinguish water levels below the peat horizon (-0.8 to -0.3 m) and within the peat horizon (-0.3 to $+0.1$ m).

mainly by radiation. This was also reported by Lindroth et al. (2007).

Water levels had a strong influence on R_{eco} fluxes ($p = 0.0004$, correlation between both: $R^2 = 0.91$; Fig. 5) as analysed by a linear mixed-effect model (Table S1 in the Supplement). A strong correlation between water table and CO₂ emissions was also observed by Silvola et al. (1996) and Berglund and Berglund (2011).

Annual NEE budgets were positively correlated to mean annual water table levels (Fig. 4b).

Peat mineralization generally increases linearly when the water table lowers (Dinsmore et al., 2009). Our study confirms this linear relationship between ecosystem respiration and water table level on a daily timescale (Fig. 5) and it could even be observed in net ecosystem exchange on an annual timescale (Fig. 4b). The increase in heterotrophic respiration may level off in dry conditions when the water table falls below the peat layer, and little extra SOC from deeper soil is exposed to aerobic conditions. On our sites, however, there was no significant difference in the relation between R_{eco} and water table when water levels were in the peat or in the subjacent sand layer. Only the water table level and the depth of the aerated soil zone affected R_{eco} but not the effective aerobic SOC stock, although the water table sometimes dropped to -30 cm below the peat layer. Consequently, peat mineralization seems to be driven by soil moisture in the topsoil rather than by peat layer depth. Deeper water levels result in drier topsoil, which is hence faster mineralized.

We confirm our hypothesis that GHG emissions of histic Gleysols (mainly CO₂) increase linearly with drainage depth but reject our hypothesis that CO₂ emissions level off when the water table falls below the peat layer.

Histic Gleysols are frequently subject to deep drainage for agriculture. Moreover, histic Gleysols tend to be more intensively used for agriculture than Histosols due to more suitable soil physical and chemical properties. Our study suggests that deeply drained histic Gleysols could be much stronger sources of GHGs than expected.

4.5 Vegetation effects

Differences in vegetation composition and biomass amounts were reflected in GPP amounts (Fig. 2). R_{eco} is not only affected by temperature, which is very similar for all sites, but also by plant biomass, which differs between sites. The assumption that plant respiration was dominating R_{eco} differences between the sites is confirmed by highly significant correlations between daily mean values of GPP and R_{eco} for each site ($p < 2.2 \times 10^{-16}$, mean $R^2 = 0.64$ for all sites). However, since the ratio of the annual R_{eco} to GPP was almost the same on all sites (mean value of 1.5 ± 0.07 ; Table 3), the influence of the vegetation on NEE of the different sites can be ruled out. Therefore, differences in NEE can be attributed to varying microbial activity as well as carbon degradation differences between the individual sites.

The C balance of all sites was clearly affected by harvest/grazing. Carbon export was as important as NEE for the annual C balance, especially on sites with high grass biomass (up to 30 percent of the C balance for site C_{low} W₂₉). In Danish permanent grassland sites, yield export had a similar contribution to the C balance as in the Grosses Moor (Elsgaard et al., 2012).

5 Conclusions

We showed that GHG emissions of histic Gleysols (mainly CO₂) increase linearly with drainage depth and do not level off when the water table falls below the peat level. Drained histic Gleysols are GHG hotspots, which have so far been neglected or underestimated.

Grasslands on histic Gleysols emit as many GHGs as grasslands on Histosols. This confirms the wide definition of organic soils for use in GHG emission inventories by IPCC (IPCC, 2006). Since shallow histic Gleysols emit as much CO₂ as deep peat soils, they should be integrated into the national and international definitions of Histosols in terms of climate-relevant carbon sources.

Peat mixed with mineral subsoil and C_{org} concentration around 10 % emits as much GHG as unmixed peat soil (> 30 % C_{org}). This implies that peat mixing with underlying sand is not a GHG mitigation option.

Supplementary material related to this article is available online at <http://www.biogeosciences.net/11/749/2014/bg-11-749-2014-supplement.pdf>.

Acknowledgements. The “Organic soils” joint research project funded by the Thünen Institute and its twelve participating research institutes aims at closing the data gap by monitoring emissions from eleven catchments in Germany. Various peatlands, differing in preservation and utilization, are investigated in order to derive specific emission factors.

- HU Berlin, especially N. Roskopf, for soil identification and soil properties.
- M. Hunziger and D. Olbrich for help during the measurement campaigns and in the lab.
- K. Gilke, R. Lausch, A. Oehns-Rittgerodt for laboratory assistance.
- S. Belting for plant species knowledge.
- DWD for climate data of stations Braunschweig, Uelzen, Wittingen-Vorhop and Wolfsburg (Südwest).
- Schäferei Paulus and Mr Horny for research permission.
- The peat group of the Thünen Institute of Climate-Smart Agriculture (B. Tiemeyer, E. Frahm, U. Dettmann, S. Frank, M. Bechtold, T. Leppelt) for discussions.

Edited by: B. Tiemeyer

References

- Alm, J., Talanov, A., Saarnio, S., Silvola, J., Ikkonen, E., Aaltonen, H., Nykanen, H., and Martikainen, P. J.: Reconstruction of the carbon balance for microsites in a boreal oligotrophic pine fen, Finland, *Oecologia*, 110, 423–431, 1997.
- Alm, J., Shurpali, N. J., Tuittila, E.-S., Laurila, T., Maljanen, M., Saarnio, S., and Minkkinen, K.: Methods for determining emission factors for the use of peat and peatlands – flux measurements and modelling, *Boreal Environ. Res.*, 12, 85–100, 2007.
- Beetz, S., Liebersbach, H., Glatzel, S., Jurasinski, G., Buczko, U., and Höper, H.: Effects of land use intensity on the full greenhouse gas balance in an Atlantic peat bog, *Biogeosciences*, 10, 1067–1082, doi:10.5194/bg-10-1067-2013, 2013.
- Bellisario, L. M., Moore, T. R., and Bubier, J. L.: Net ecosystem CO₂ exchange in a boreal peatland, northern Manitoba, *Ecoscience*, 5, 534–541, 1998.
- Berglund, O. and Berglund, K.: Influence of water table level and soil properties on emissions of greenhouse gases from cultivated peat soil, *Soil Biol. Biochem.*, 43, 923–931, 2011.
- Blodau, C.: Carbon cycling in peatlands: A review of processes and controls, *Environ. Rev.*, 10, 111–134, 2002.
- Boden, A.-H.-A.: *Bodenkundliche Kartieranleitung* (Soil survey manual), 5th Edn., Dienst, B. f. G. u. R. i. Z. m. d. S. G., Hannover, 2005.
- Burnham, K. P. and Anderson, D. R.: Multimodel Inference: Understanding AIC and BIC in Model Selection, *Sociological Methods & Research*, 33, 261–304, 2004.
- Dinsmore, K. J., Skiba, U. M., Billett, M. F., and Rees, R. M.: Effect of water table on greenhouse gas emissions from peatland mesocosms, *Plant Soil*, 318, 229–242, 2009.
- Don, A., Rödenbeck, C., and Gleixner, G.: Unexpected control of soil carbon turnover by soil carbon concentration, *Environ. Chem. Lett.*, 11, 407–413, doi:10.1007/s10311-013-0433-3, 2013.

- Drösler, M.: Trace gas exchange and climatic relevance of bog ecosystems, Southern Germany, Lehrstuhl für Vegetationsökologie, Departement Ökologie, TUM, München, 179 pp., 2005.
- Drösler, M., Freibauer, A., Christensen, T. R., and Friborg, T.: Observations and status of peatland greenhouse gas emissions in Europe, in: *The continental-scale greenhouse gas balance of Europe*, edited by: Dolman, A. J., Freibauer, A., and Valentini, R., Springer, New York, 243–261, 2008.
- Drösler, M., Adelman, W., Augustin, J., Bergmann, L., Beyer, C., Chojnicki, B., Förster, C., Freibauer, A., Giebels, M., Görlitz, S., Höper, H., Kantelhardt, J., Liebersbach, H., Hahn-Schöfl, M., Minke, M., Petschow, U., Pfadenhauer, J., Schaller, L., Schägner, P., Sommer, M., Thuille, A., and Wehrhan, M.: Klimaschutz durch Moorschutz. Schlussbericht des Vorhabens “Klimaschutz – Moorschutzstrategien”, 2006–2010, 2013.
- Efron, B.: Bootstrap methods: Another look at the jackknife, *Ann. Stat.*, 7, 1–26, 1979.
- Elsgaard, L., Gorres, C.-M., Hoffmann, C. C., Blicher-Mathiesen, G., Schelde, K., and Petersen, S. O.: Net ecosystem exchange of CO₂ and carbon balance for eight temperate organic soils under agricultural management, *Agr. Ecosyst. Environ.*, 162, 52–67, 2012.
- Falge, E., Baldocchi, D., Olson, R., Anthoni, P., Aubinet, M., Bernhofer, C., Burba, G., Ceulemans, R., Clement, R., Dolman, H., Granier, A., Gross, P., Grunwald, T., Hollinger, D., Jensen, N. O., Katul, G., Keronen, P., Kowalski, A., Lai, C. T., Law, B. E., Meyers, T., Moncrieff, H., Moors, E., Munger, J. W., Pilegaard, K., Rannik, U., Rebmann, C., Suyker, A., Tenhunen, J., Tu, K., Verma, S., Vesala, T., Wilson, K., and Wofsy, S.: Gap filling strategies for defensible annual sums of net ecosystem exchange, *Agr. Forest Meteorol.*, 107, 43–69, 2001.
- Forster, P., Ramaswamy, V., Artaxo, P., Bernsten, T., Betts, R., Fahey, D. W., Haywood, J., Lean, J., Lowe, D. C., Myhre, G., Nanga, J., Prinn, R., Raga, G., Schulz, M., and Van Dorland, R.: Changes in Atmospheric Constituents and in Radiative Forcing. In: *Climate Change 2007: The Physical Science Basis. Contribution of Working Group I to the Fourth Assessment Report of the Intergovernmental Panel on Climate Change*, edited by: Solomon, S., Qin, D., Manning, M., Chen, Z., Marquis, M., Averyt, K. B., Tignor, M., and Miller, H. L., Cambridge University Press, Cambridge, United Kingdom and New York, NY, USA, 2007.
- Göttlich, K.: *Moor- und Torfkunde (Peatland and peat knowledge)*, Stuttgart, E. Schweizerbart'sche Verlagsbuchhandlung (Nägele und Obermiller), 1990.
- HBU: Handbook of soil analyses (HBU), Soil quality – Determination of dry bulk density Berlin, Beuth Verlag GmbH, ISO 11272, 10 pp., 1998.
- HBU: Handbook of soil analyses (HBU), Soil quality – Determination of pH, Berlin, Beuth Verlag GmbH, ISO 10390, 9 pp., 2005.
- Huber, P. J.: *Robust Statistics*, J. Wiley, New York, 1981.
- IPCC: Guidelines for National Greenhouse Gas Inventories, Chapter 3: Consistent Representation of Lands, 2006.
- Klemetsson, L., von Arnold, K., Weslien, P., and Gundersen, P.: Soil CN ratio as a scalar parameter to predict nitrous oxide emissions, *Glob. Change Biol.*, 11, 1142–1147, 2005.
- Kottek, M., Grieser, J., Beck, C., Rudolf, B., and Rubel, F.: World Map of the Köppen-Geiger climate classification updated, *Meteorol. Z.*, 15, 259–263, 2006.
- Kruijt, B., Elbers, J. A., von Randow, C., Araujo, A. C., Oliveira, P. J., Culf, A., Manzi, A. O., Nobre, A. D., Kabat, P., and Moors, E. J.: The robustness of eddy correlation fluxes for Amazon rain forest conditions, *Ecol. Appl.*, 14, S101–S113, 2004.
- Lai, D. Y. F.: Methane dynamics in northern peatlands: a review, *Pedosphere*, 19, 409–421, 2009.
- Limpens, J., Berendse, F., Blodau, C., Canadell, J. G., Freeman, C., Holden, J., Roulet, N., Rydin, H., and Schaepman-Strub, G.: Peatlands and the carbon cycle: from local processes to global implications – a synthesis, *Biogeosciences*, 5, 1475–1491, doi:10.5194/bg-5-1475-2008, 2008.
- Lindroth, A., Lund, M., Nilsson, M., Aurela, M., Christensen, T. R., Laurila, T., Rinne, J., Riutta, T., Sagerfors, J., Stroem, L., Tuovinen, J.-P., and Vesala, T.: Environmental controls on the CO₂ exchange in north European mires, *Tellus B*, 59, 812–825, 2007.
- Lloyd, J. and Taylor, J. A.: On the temperature dependence of soil respiration, *Funct. Ecol.*, 8, 315–323, 1994.
- Londo, G.: Decimal scale for relevés of permanent quadrats, *Vegetatio*, 33, 61–64, 1976.
- Marschner, B., Brodowski, S., Dreves, A., Gleixner, G., Gude, A., Grootes, P. M., Hamer, U., Heim, A., Jandl, G., Ji, R., Kaiser, K., Kalbitz, K., Kramer, C., Leinweber, P., Rethemeyer, J., Schaeffer, A., Schmidt, M. W. I., Schwark, L., and Wiesenberger, G. L. B.: How relevant is recalcitrance for the stabilization of organic matter in soils?, *J. Plant Nutr. Soil Sc.*, 171, 91–110, doi:10.1002/jpln.200700049, 2008.
- Mikutta, R., Kleber, M., Torn, M., and Jahn, R.: Stabilization of Soil Organic Matter: Association with Minerals or Chemical Recalcitrance?, *Biogeochem.*, 77, 25–56, doi:10.1007/s10533-005-0712-6, 2006.
- Montanarella, L., Jones, R. J. A., and Hiederer, R.: The distribution of peatland in Europe, *Mires Peat*, 1, 1–11, 2006.
- Nielsen, O.-K., Mikkelsen, M. H., Hoffmann, L., Gyldenkerne, S., Winther, M., Nielsen, M., Fauser, P., Thomsen, M., Plejdrup, M. S., Albrektzen, R., Hjelgaard, K., Bruun, H. G., Johannsen, V. K., Nord-Larsen, T., Bastrup-Birk, A., Vesterdal, L., Møller, I. S., Rasmussen, E., Arfaoui, K., Baunbæk, L., and Hansen, M. G.: Denmark's National Inventory Report 2012, Emission Inventories 1990–2010 – Submitted under the United Nations Framework Convention on Climate Change and the Kyoto Protocol, Aarhus University, DCE – Danish Centre for Environment and Energy, 1168 pp., Scientific Report from DCE No. 19., available at: <http://www.dmu.dk/Pub/SR19.pdf>, 2012.
- Oberdorfer, E.: *Pflanzensoziologische Exkursionsflora für Deutschland und angrenzende Gebiete*, 8th Edn., Verlag Eugen Ulmer, Stuttgart, 2001.
- Overbeck, F.: Das Große Moor bei Gifhorn im Wechsel hydrokliner und xerokliner Phasen der nordwestdeutschen Hochmoorentwicklung [The “Großes Moor” near Gifhorn during the alternation of hydrocline and xerocline periods of the northwestern German peat bog development], Walter Dorn Verlag, Bremen, 1952.
- Pedersen, A. R., Petersen, S. O., and Schelde, K.: A comprehensive approach to soil-atmosphere trace-gas flux estimation with static chambers, *Eur. J. Soil Sci.*, 61, 888–902, 2010.
- Petersen, S. O., Hoffmann, C. C., Schäfer, C.-M., Blicher-Mathiesen, G., Elsgaard, L., Kristensen, K., Larsen, S. E., Torp, S. B., and Greve, M. H.: Annual emissions of CH₄ and N₂O,

- and ecosystem respiration, from eight organic soils in Western Denmark managed by agriculture, *Biogeosciences*, 9, 403–422, doi:10.5194/bg-9-403-2012, 2012.
- Pinheiro, J., Bates, D., DebRoy, S., Sarkar, D., and Team, R. D. C.: Linear and nonlinear mixed effect models, R package version 3.1-108, 2013.
- R Core Team, R. C.: R: A language and environment for statistical computing, available at: <http://www.R-project.org/>, 2012.
- Reiche, M., Gleixner, G., and Küsel, K.: Effect of peat quality on microbial greenhouse gas formation in an acidic fen, *Biogeosciences*, 7, 187–198, doi:10.5194/bg-7-187-2010, 2010.
- Richter, A.: Bodenübersichtskarte der Bundesrepublik Deutschland – BÜK 1000 (Soil survey map), 2nd Edn., 1998.
- Rousseeuw, P., Croux, C., Todorov, V., Ruckstuhl, A., Salibian-Barrera, M., Verbeke, T., Koller, M., and Maechler, M.: robustbase: Basic Robust Statistics, R package version 0.9-4, available at: <http://CRAN.R-project.org/package=robustbase> (last access: 24 April 2013), 2012.
- Schäfer, C. M., Elsgaard, L., Hoffmann, C. C., and Petersen, S. O.: Seasonal methane dynamics in three temperate grasslands on peat, *Plant Soil*, 357, 339–353, 2012.
- Schrier-Uijl, A. P., Kroon, P. S., Hensen, A., Leffelaar, P. A., Berendse, F., and Veenendaal, E. M.: Comparison of chamber and eddy covariance-based CO₂ and CH₄ emission estimates in a heterogeneous grass ecosystem on peat, *Agr. Forest Meteorol.*, 150, 825–831, 2010.
- Silvola, J., Alm, J., Ahlholm, U., Nykanen, H., and Martikainen, P. J.: CO₂ fluxes from peat in boreal mires under varying temperature and moisture conditions, *J. Ecol.*, 84, 219–228, doi:10.2307/2261357, 1996.
- Smith, K. A. and Conen, F.: Impacts of land management on fluxes of trace greenhouse gases, *Soil Use Manage.*, 20, 255–263, doi:10.1079/sum2004238, 2004.
- Thomas, K. L., Benstead, J., Davies, K. L., and Lloyd, D.: Role of wetland plants in the diurnal control of CH₄ and CO₂ fluxes in peat, *Soil Biol. Biochem.*, 28, 17–23, doi:10.1016/0038-0717(95)00103-4, 1996.
- UBA: National Inventory Report for the German Greenhouse Gas Inventory 1990 – 2010, Submission under the United Nations Framework Convention on Climate Change and the Kyoto Protocol 2012, Dessau, Germany, 2012.
- VDLUFa: Bestimmung von mineralischem (Nitrat-)Stickstoff in Bodenprofilen (Nmin-Labormethode), in: *Methodenbuch Teil 2*, VDLUFa, Speyer, Germany, 1997.
- Woodward, F. I. and Lomas, M. R.: Vegetation dynamics – simulating responses to climatic change, *Biol. Rev.*, 79, 643–670, 2004.
- WRB: World Reference Base for Soil Resources 2006, Ein Rahmen für internationale Klassifikation, Korrelation und Kommunikation, Deutsche Ausgabe, Bundesanstalt für Geowissenschaften und Rohstoffe, Hannover, 2008.